Micromechanical Broadband Infrared Sensors based on Piezoelectric Bending Resonators

Xiaoqi Bao[1]*, Stewart Sherrit[1], Clifford F. Frez[1], and Mina Rais-Zadeh[1,2]
[1] Jet Propulsion Laboratory, California Institute of Technology, Pasadena, CA 91109, USA
[2] Department of Electrical Engineering, University of Michigan, Ann Arbor, MI 48109, USA

ABSTRACT

There is a high demand for high-performance and low-cost uncooled infrared (IR) detectors. In order to meet this need we are investigating the use of MEMS piezoelectric resonator technology using aluminum nitride (AlN) thin films. Recent research has shown that piezoelectric resonators have the potential to be used as a core element for highly sensitive, low-noise, and low-power uncooled IR detectors. A novel design of an AlN IR sensor based on piezoelectric bending resonator is described and analyzed in this paper. The detector is constructed by using thermally mismatched materials which stress the resonator and shift the resonance frequency. The IR thermal input is sensed by monitoring the frequency shift induced by the in-plan thermal stress. These designs have the potential for very high sensitivity and are compatible with commercially viable CMOS fabrication technology.

KEYWORD: MEMS, IR sensor, piezoelectric resonators, bending mode.

1. INTRODUCTION

Uncooled IR detectors have applications from medical, terrestrial and military to space imaging science instruments. Microelectromechanical resonators having high quality factors (*Q*s) have recently been used as the detector pixel for IR imagers [1] – [3]. Uncooled IR detection, *i.e.* the ability to perform imaging without the need to cool the detector pixels, is another advantage of resonant MEMS detectors that results in significant size and power reduction. IR sensors using gallium nitride (GaN) [1], [2], aluminum nitride (AlN) [3], [4] or barium strontium titanate (BST) based resonators [5] have been reported previously. One of the main parameters of resonant detectors that directly translates to high sensitivity detection is the temperature coefficient of frequency (TCF). Typical TCF values of AlN, AlN-on-silicon or GaN in-plan vibration mode resonators previously reported are ~ -30 ppm/K, where TCE is its main contributor [1]-[4].

In this work, we conceived a new configuration of the resonator to achieve high TCF values not limited by the temperature coefficient of elasticity (TCE) of the materials in the resonating stack. The novel MEMS IR sensor consists of a piezoelectric bending resonator with a frame made of a material having a high mismatch coefficient of thermal expansion (CTE). As is well known, bending resonance frequencies of thin plates are determined by the mass density and bending stiffness as well as in-plan stress [6]. A tensional in-plan stress will increase the resonance frequency and, conversely, a compressional in-plan stress decreases the frequency. A large thermal mismatch

[1]* Correspondence: xbao@jpl.nasa.gov

between the materials in the frame and in the resonating stack can create a large thermal stress and induce a large frequency change of >1000 ppm/K.

The top surface of the resonator is covered by an IR absorber material. The resonator is connected to the silicon substrate (thermal heat sink) through thin tethers. The basic sensing mechanism of the sensor is 1) the energy of the incident IR radiation results in a temperature rise of the sensor. 2) The temperature change induces an in-plan thermal stress in the resonator by the CTE mismatch between the plate and the frame. 3) The thermal stress changes the bending rigidity of the resonator and results in a resonance frequency change. 4) The shift in the frequency is readout by suitable electronics through the electrodes on the piezoelectric films [4], [7-8]. The frequency shift is related to the input IR power.

A schematic of one of the MEMS IR sensor designs is presented in **Figure 1** with the top view in the left figure and a CMOS technology compatible layer stack in the right figure. It uses circular bimorph resonator having two piezoelectric layers of AlN. The CTE mismatching ring is made of zinc which has a large CTE of ~39×10^{-6} compared to ~4.2×10^{-6} of AlN. The IR absorber layer is made of silicon nitride (SiN). The tether has the same stack as the center part of the resonator except for the SiN layer.

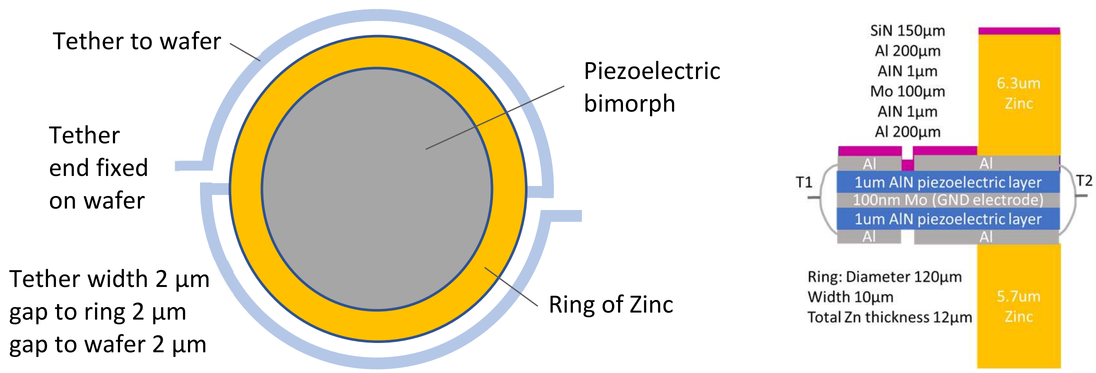

Figure 1: Schematic of an IR sensor design using piezoelectric bending resonator (not scaled).

2. FE SIMULATION

The performances of the IR sensors based on the described mechanism were evaluated by Finite Element (FE) modeling. **Figure 2** shows the FE model of the design described by **Figure 1**. A design parameter study was performed for the sensors to evaluate the performance. The TCF of the first bending mode was evaluated for different total thickness values of the ring. In the evaluation we first calculated the frequency in the case where there is no in-plan stress. Then, the thermal stress due to a specific temperature change was added and the frequency shift was calculated as a result of the thermal stress. The TCF was calculated as

$$\mathrm{TCF} = \Delta f_r / f_r / \Delta \mathrm{T}, \quad (1)$$

where f_r is initial resonance frequency, T is the temperature and the Δf_r indicates the difference between the initial resonance frequency and the frequency after the application of the temperature change.

The first bending mode (the (0, 0) mode of circular plate) of a resonator with the dimensions marked in **Figure 1** is shown in **Figure 3 (a)**. With a total ring thickness of 12 μm, the resonance frequency is 3.42 MHz. **Figure 3(b)** shows the static deformation of the resonator as the temperature is raised by 10 °C. The ring expanded and applied tensional stress to the center part of the resonator. The averaged stress is 21.3 MPa.

Usually piezoelectric resonators are characterized experimentally by network analyzers, which measure the transmission spectrum. In order to compare the simulation results with the experimental data, the transmission spectrums for 50-Ohm transmission line were computed by the model. The electrode pattern and connection are determined by the mode shape for a high electromechanical coupling. For the particular design shown here, the electric charges has opposite signs on the center and surrounding area due to the stress distribution of the mode (see **Figure 3(a)**). Both top and bottom electrodes are divided according to the charge signs. The terminal 1 (T1) is connected to both top and bottom center areas and the T2 to the surrounding area (see **Figure 1**). The *Q* factor of the microfabricated AlN film is in a range of 1000 – 10,000. A mechanical *Q* of 1000 was assumed in our computation. The calculated spectrum is presented in the left of **Figure 4** as well as a schematic drawing of the transmission line in the right where the resonator is represented by a Van Dyke model.

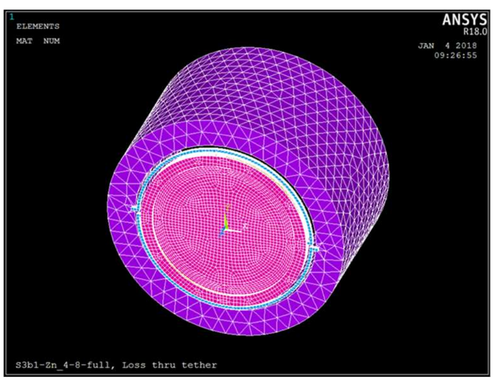

Figure 2: FE model of the IR sensor.

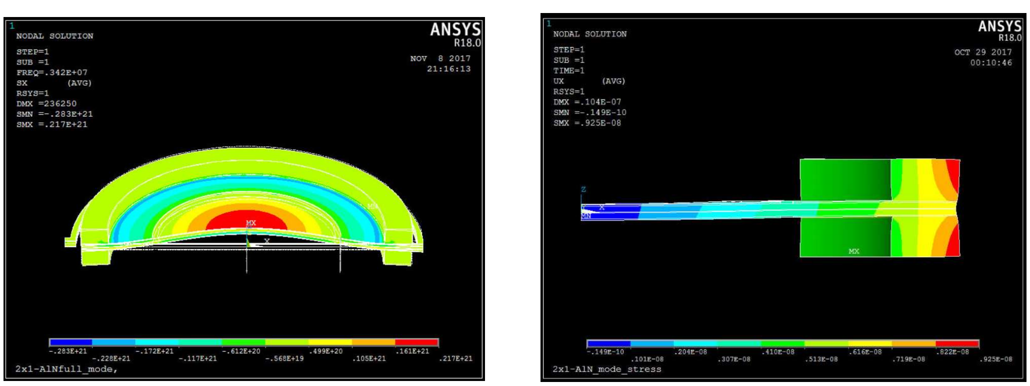

(a) **(b)**

Figure 3: (a) Deformation and stress distribution in radial direction of the first bending vibration mode (3.42 MHz) of a resonator design. (b) Deformation and in-plan stress in radial direction with ΔT of +10°C.

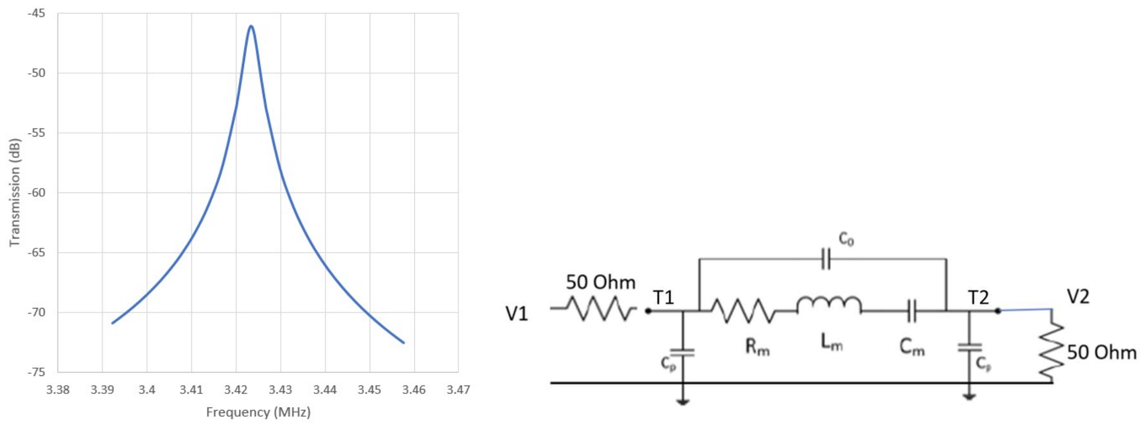

Figure 4: A transmission spectrum of the resonator (Q_m = 1000) with a 50-Ohm line.

A design parameter study was performed for different total thickness values of the ring in the range of 1 – 12 µm while the width was fixed at 10 µm for resonators of 120 µm in diameter and the layer stack as shown in **Figure 1**. The results are summarized in **Figure 5** as a function of the Zinc total thickness. The predicted TCF is over 1000 ppm/K when the total zinc thickness is more than 3 µm. The thermal stress in the center (thin) part of the resonator increases with the thickness almost linearly in the computed range. The TCF also increases with the thickness but the rate decreases and starts to saturate at higher thickness values. It should be noted that the thicker zinc will result in a larger thermal capacitor of the resonator, which means more IR energy is needed to raise the temperature by the same amount. A tradeoff is required to obtain the best performance for a particular application, and a thermal analysis is needed in the trade study.

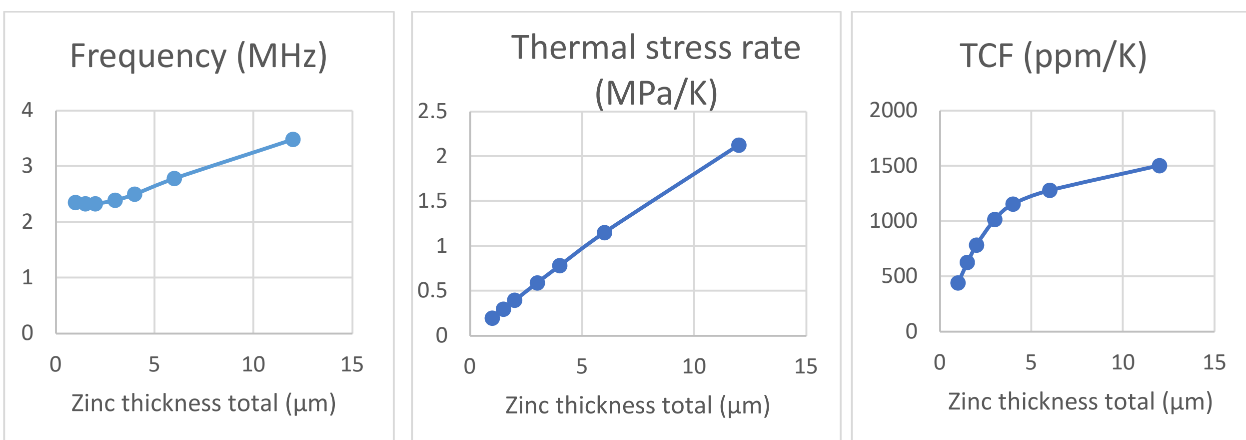

Figure 5: Frequency, in-plan thermal stress, and TCF vs. zinc ring thickness with width of 10 µm.

We applied both analytical and FE models for the thermal analyses. In the analytical model, we treat the resonator as a thermal capacitor, c, and the tethers as a thermal resistor, r, while assuming the temperature at the interface of the tether end and wafer maintains constant at T_0, during the sensing period. The temperature of the resonator is expressed as

$$T = T_0 + Pr(1 - e^{-(t/\tau)}), \quad (2)$$

for IR radiation turn on period, where P is the absorbed power and τ is the time constant that equals to rc. The initial temperature of the resonator is T_0. And,

$$T = T_0 + (T_1 - T_0)\, e^{-(t/\tau)} \quad (3)$$

for IR radiation turn off period, where T_1 is the initial temperature of the resonator.

The FE thermal model includes a large silicon volume to model and represent the thermal heat sink (the silicon substrate). Estimations show that the radiation and convection loss at room temperature are neglectible compared with the solid conduction through the tether in our case. Only thermal conductions are therefore modeled.

Figure 6 shows both FE and the analytical model for an investigated design. The two results are in good agreement. This implies that the analytical model is a good representation of the system and can be used to iterate for most of our designs.

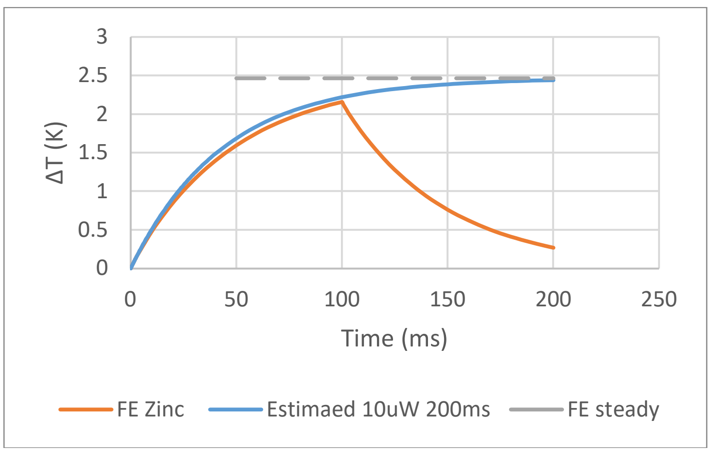

Figure 6: The temperature response of 10 μW IR input.

We used the analytical thermal model to evaluate the overall performance for given IR power inputs. According to Eq. (2), the steady state Power Coefficient of Frequency (PCF) is expressed as

$$\mathrm{PCF} = (\Delta f_r/f_r)/p|_{t=\infty} = r\mathrm{TCF} \quad (4)$$

Therefore, for the applications allowing long observation time, higher TCF resonator designs with higher thermal resistance tethers will have higher frequency shift.

For the applications where the time response is critical, say requiring a short time constant of τ_0, we need to design the thermal resistance of the tethers for the resonator to satisfy the response time requirement, we therefore have

$$r = \tau_0/c, \quad (5)$$

and

PCF = τ_0 (TCF/c). (6)

Eq. 6 shows the sensitivity PCF for a given τ_0 is proportional to TCF/c. Therefore, the constant of TCF/c can be considered as a figure of merit of the resonator designs for these applications. This figure of merit was applied to the resonator design parameter study. As shown in **Figure 7(a)**, the maximum of TCF/c is found at a zinc thickness of ~ 4 µm. At this point, we can achieve a maximum PCF for a given time constant. The achievable PCF as a function of time constant is shown in **Figure 7(b)**.

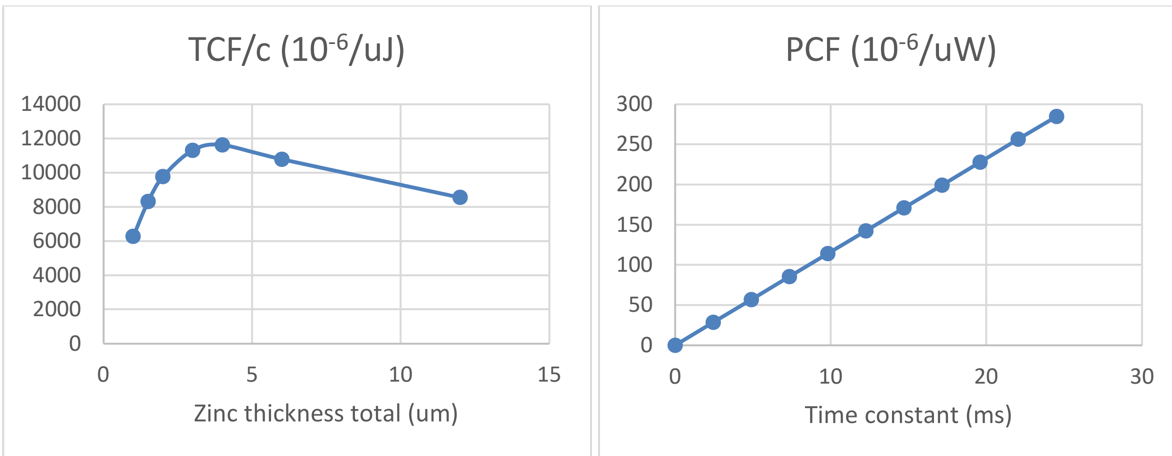

(a) (b)

Figure 7: (a) The figure of merit vs. zinc thickness and (b) PCF of resonator with 4 µm zinc vs. time constant.

Low loss or correspondingly high mechanic Q is important for a high sensitivity and low power readout. The loss of the vibration energy caused by mechanic coupling of resonator with the silicon wafer through the tether connections (also known as the anchor or support loss) was investigated by FE simulation. We artificially set losses of all materials in the resonating stack to zero and add a large damping to the silicon substrate material to absorb the elastic wave in a limited modeled volume to mimic a relatively large wafer. We found the thin and relatively soft tethers in our designs usually only induce a small additional loss corresponding to a $Q_{\text{anchor}} > 25{,}000$. It is insignificant compared to the intrinsic material loss of the AlN film. The Q of the later is in a range of 1000 – 10,000. However, when the tether has a resonance frequency close to the frequency of the resonator, strong coupling between them can occur. The strong coupling can split one resonator mode to two modes and induce a large damping. This phenomenon was observed in our study. An example is shown in **Figure 8**. The resonator without tether connection has a (0, 0) mode at 2.348 MHz. With the tethers connecting to wafer and having a flexural resonance frequency matching the resonance of the main disc, we get two modes at 2.297 MHz and 2.395 MHz instead of one. As shown in the figure, the vibration amplitude in the tethers is much stronger than that in the resonator. The anchor Qs of the two modes are only 600 and 650, respectively. Such a mode coupling should be avoid in the designs. A convenient way to fix the problem is to change the length of the tethers.

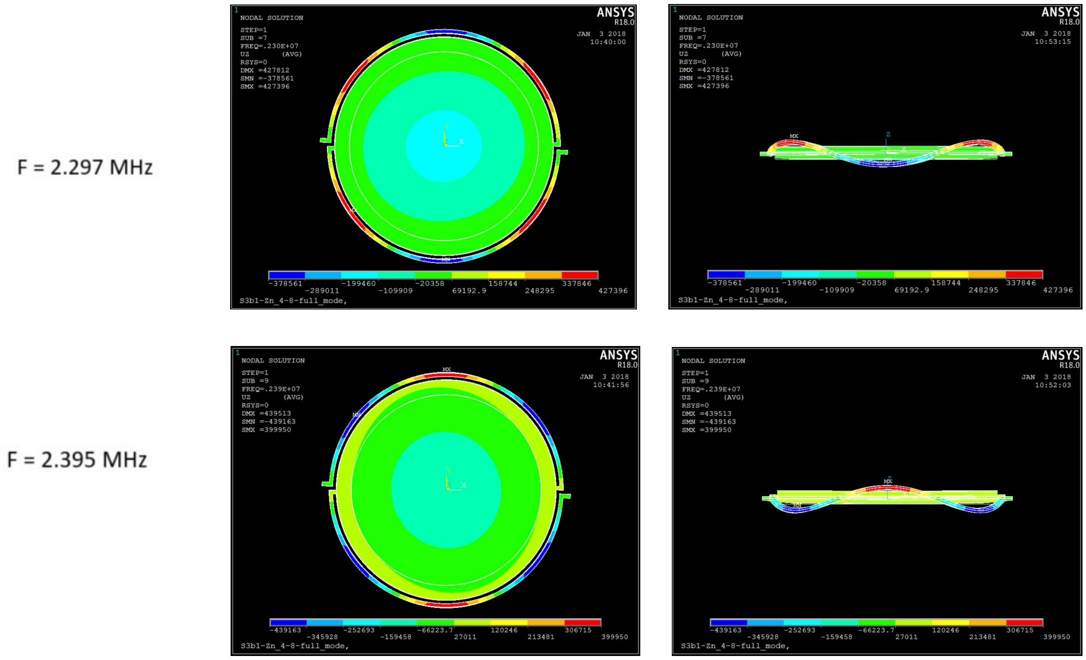

Figure 8: Out-plan displacement of split modes due to mode coupling between the tethers and the resonator

Combining the thermal and resonance analysis the overall performances were predicted. The results of the design of **Figure 1** are summarized in **Table 1**. The TCF of the sensor is more than 10 time larger than the sensors based on in-plan (longitudinal) resonator. This suggests that a high sensitivity to the IR power is achievable with a proper thermal design.

Table 1: Summary of IR sensor performance.

Frequency	Q_{anchor}	**Thermal Capacity**	**Thermal Conductance**	**Time Constant**	**Temperature/ Power**	**Thermal Stress rate**	**TCF**	**PCF**	**Frequency Sensitivity**
MHz	-	μJ/K	μW/K	ms	K/μW	MPa/K	10^{-6}/K	10^{-6}/μW	kHz/μW
3.42	67,000	0.176	4.06	43.38	0.247	2.13	1504	370.8	1.29

3. SUMMARY

A novel design of an AlN IR MEMS sensor based on piezoelectric bending resonator is described and analyzed in this paper. The detector is constructed using a frame made of thermally mismatch materials to stress the resonator plate and shift the resonance frequency. The IR thermal input is sensed by monitoring the frequency shift induced by the in-plan thermal stress. The FE analysis show this design can achieve a high TCF (1500 ppm/K) which is more than 10 times the sensitivity of sensors based on in-plane vibration (longitudinal) resonator.

Porotype IR sensors based on the described mechanism will be fabricated in the near future to verify the modeling results.

4. ACKNOWLEDGMENT

Research reported in this manuscript was conducted at the Jet Propulsion Laboratory (JPL), California Institute of Technology, under a contract with National Aeronautics Space Administration (NASA).

5. REFERENCES

[1] V. J. Gokhale, J. Roberts, and M. Rais-Zadeh, “Sensitive uncooled IR detectors using gallium nitride resonators and silicon nitride absorbers,” *Hilton Head Workshop*, Hilton Head, SC, pp. 46-49, June, 2012.

[2] V. J. Gokhale, Y. Sui, and M. Rais-Zadeh, “Novel uncooled detector based on gallium nitride micromechanical resonators,” *SPIE Defense, Security, and Sensing*, 2012, pp. 835319-835319-6.

[3] V. Gokhale, C. Figueroa, J. M. L. Tsai, and M. Rais-Zadeh, “Low-noise AlN-on-Si resonant infrared detectors using a commercial foundry MEMS fabrication process,” *IEEE MEMS Conf*., pp. 73-76, Jan. 2015.

[4] M. Moosavifar, A. Ansari, and M. Rais-Zadeh,” An AlN-on-Si resonant IR sensor array with a large temperature coefficient of frequency,” *15th IEEE Sensors Conference*, pp. 1-3, SENSORS 2016

[5] M. Z. Koohi, S. Lee, V. Lee, S. Ahmet Sis, and A. Mortazawi,” Un-cooled resonant IR detectors based on barium strontium titanate switchable FBARs,” *European Microwave Conf*., 2015, pp. 948-951.

[6] Wah, Thein, “Vibration of Circular Plates,” JASA, vol. 34, no. 3, Mar., pp. 275-281 (1962).

[7] H. Jiang et al, “A 30 ppm < 80 nJ ring-down-based readout circuit for resonant sensors,” *IEEE J. Solid-State Circuits*, pp. 187-195, Jan 2016.

[8] Yu Hui, and M. Rinaldi, “Aluminum nitride nano-plate infrared sensor with self-sustained CMOS oscillator for nano-Watts range power detection,” *IFCS*, 2013, pp. 62-65.